ORIGINAL RESEARCH

Temperature-dependent storage modulus of polymer nanocomposites, blends and blend-based nanocomposites based on percolation and De Gennes's self-similar carpet theories

Reza Mohammadi[1,2] · Esmail Sharifzadeh[1,2] · Neda Azimi[3]

Abstract

Temperature-dependent storage modulus of polymer nanocomposites, blends and blend-based nanocomposites was studied using both analytical and experimental approaches. The analytical strategy comprised modeling the thermomechanical property of the systems based on parameters affecting the conversion degree of polymer chains in state-to-state transitions and mechanical characteristics of the polymer/polymer interface. Accordingly, percolation theory was developed to define the order of conversion rate and conversion degree of polymer chains considering the thermomechanical characteristics of the neat polymer matrix, behavior of nanoparticles in the system and formation of polymer/particle interphase region. The effect of interphase on a temperature-dependent conversion of polymer molecules was estimated based on De Gennes's self-similar using the molecular characteristics of the adsorbed polymer chains and related scaling factor. To validate the model predictions, different neat, blend, nanocomposite and blend-based nanocomposite samples were prepared using high-density polyethylene, polyethylene terephthalate and hollow graphene oxide nanoparticles, where needed, and subjected to dynamic mechanical thermal analysis and other required tests. Besides providing acceptably accurate predictions in the case of all neat and nanocomposite samples, the model was proved to be independent of the system's morphological variation.

✉ Esmail Sharifzadeh
  E.sharifzadeh@razi.ac.ir

1 Department of Chemical Engineering, Faculty of Petroleum and Chemical Engineering, Razi University, Kermanshah, Iran

2 Polymer Research Division, Advanced Chemical Engineering Research Center, Razi University, Kermanshah, Iran

3 CFD Research Division, Advanced Chemical Engineering Research Center, Razi University, Kermanshah, Iran

Graphical abstract
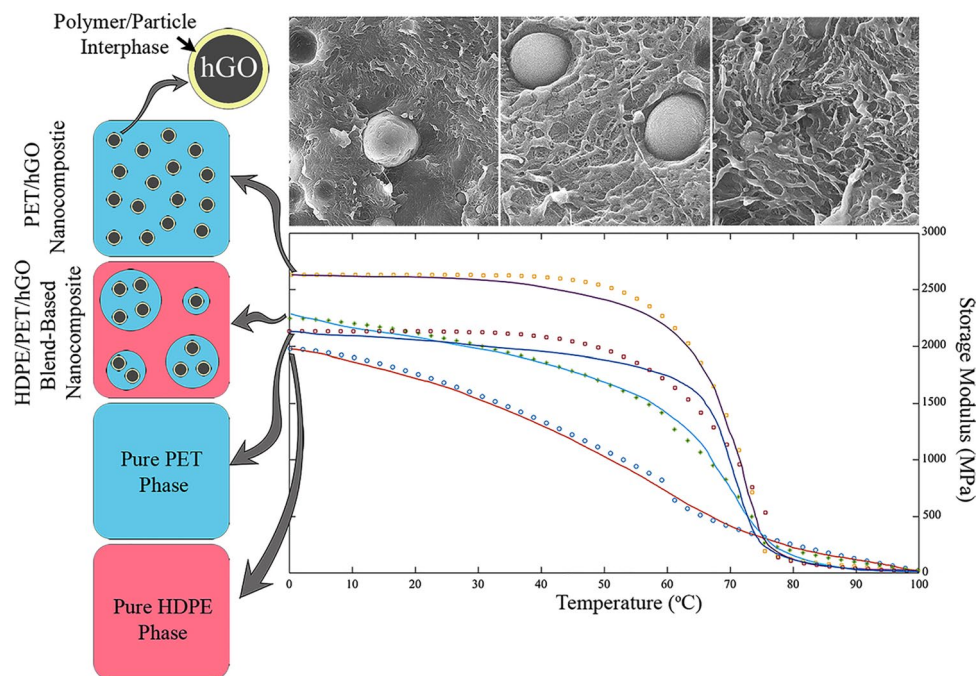
Keywords Thermomechanical properties · Nanocomposites · Blends · Compatibilization · Interface

Introduction

Polymer materials are well-known for their wide domestic and industrial applications due to relatively simple processability, low weight, high durability in hostile environments, availability, etc. [1, 2]. The physical/mechanical characteristics of polymers can be manipulated by controlling their molecular structure [3]. For instance, increasing the crystallinity percentage in semi-crystalline polymers directly affects the density, storage modulus and strength, thermal conductivity, yield strength and other parameters that are determinative in defining whether or not a specific polymer material is suitable for a particular service [4–6]. Meanwhile, other strategies have been considered as efficient approach to change the physical/mechanical characteristics of this family of materials to adapt them to specific processing/manufacturing conditions [7, 8]. Among these methods, the application of a second phase is the most common one which includes adding polymer or different size mineral reinforces to a continuous (major) polymer phase [7, 9]. Clearly, the interaction between phases, however different in polymer blends and composites, can substantially alter the characteristics of the system and make it possible to produce engineered products [10, 11].

Polymers are mostly immiscible, due to their different molecular structure and characteristics, which makes it essential to adopt specific approaches to enhance the properties of the polymer/polymer interface [12, 13]. The application of specific compatibilizers or grafting chemical functions/groups onto the polymer chains are proven to be practical however, they cannot be applied to all blending systems [12]. Adding different-sized mineral particles, especially nanoparticles, has proved to be a very useful strategy to increase the compatibility at the polymer/polymer interface in polymer blends [12, 14]. It is the nature of the reinforcing particle (e.g., polar or/and non-polar) that determines their localization in either phase or at the polymer/polymer interface [13, 15]. Many efforts have been dedicated to synthesizing micro/nanoparticles with amphiphilic chemical/physical characteristics, known as Janus nanoparticles, so they can attach to immiscible polymer phases and increase their local miscibility [16]. One of the distinct advantages of using simple micro/nanoparticles in binary polymer blends, regardless of their behavior in the system, is the induction of the characteristics of composites to the system. Besides the drastic improvement of all physical/mechanical properties, this specific strategy helps to enhance the process controllability of these so-called bend-based polymer micro/nanocomposites [17, 18].

The properties of immiscible polymer blends are in direct relation with the content of the phases and system morphology [19]. Generally, by increasing the content of the minor

polymer phase before a critical point, known as "percolation threshold", its droplets start to grow independently and the system develops droplet-matrix morphology [20]. After the percolation threshold, increasing the content of the minor phase causes the droplets to coalesce and form oval-like distinct regions which grow to rod-like structures until the amount of minor phase reaches the phase inversion point where the system is assumed to have a co-continuous morphology [19]. Accordingly, between the percolation threshold and phase inversion point the system consists of different elements of the minor phase with either droplet-matrix or co-continuous morphology [19].

It is very important to mark all effective parameters and their distinct impact on the physical/mechanical characteristics of the polymer materials/structures [2, 21, 22]. For instance, the variation of temperature is proved to substantially affect the mechanical characteristics of polymers (e.g., tensile strength/modulus, yield strain, toughness, etc.) however, the material choice is commonly based on the reported data at a particular temperature [23, 24]. This is even more crucial in the case of polymer or blend-based micro/nanocomposites since the presence of the mineral reinforcing agents with relatively higher thermal conductivity, facilitates the heat distribution in the system and increases the negative impact of temperature on the physical/mechanical properties [25–27]. Moreover, besides affecting the percolation threshold in a blend, the added nanoparticles can attract polymer chains and form polymer/particle interphase [28, 29]. The quality of polymer/particle compatibility dictates their localization in major or minor phases as well as the physical/mechanical characteristics of the polymer/particle interphase [28]. It is proved that the formation of a polymer/particle interphase can even better improve the temperature distribution in nanocomposite systems containing compatible nanoparticles [30, 31]. This phenomenon intensifies the impact of the ambient temperature on the physical/mechanical properties of the system [23, 32, 33].

To better evaluate this subject, in the present study, the temperature-dependent storage modulus of neat polymers, nanocomposites, blends and blend-based nanocomposites (BBNs) was investigated in a specific temperature range. It was considered that the nanoparticles were dispersed in either major or minor polymer phase and accordingly, the impact of the variation of temperature, content of system constituents, polymer/particle interphase and/or polymer/polymer interface on the storage modulus of the system was carefully defined. At first, the temperature-dependent storage modulus of different phases, with/without nanoparticles, was determined separately and the obtained results were combined, in the case of blend and BBN samples, using a specific form of rule of mixtures including the impact of polymer/polymer interface. The content of the polymer/particle interphase was estimated using the developed De Gennes's self-similar carpet theory

and the molecular characteristics of the polymer matrix. Also, a specific approach was developed to evaluate the impact of the content of nanoparticles on the percolation threshold of the polymer minor phase. Neat polymer, nanocomposite, blend and BBN samples, with/without synthesized spherical hollow graphene oxide (hGO) nanoparticles, were prepared using polyethylene terephthalate (PET) and high-density polyethylene (HDPE) and subjected to dynamic mechanical thermal analysis (DMTA) whose results were used to validate the model predictions. Different amounts of hGO (1–3% by vol) and minor polymer phase ($\cong$ 10–50% by vol) were used in the samples to cover the likely morphological variations, investigated using field emission scanning electron microscopy (FE-SEM). Besides providing accurate predictions in the case of all neat, nanocomposite, blend and BBN samples the model represented useful information regarding the molecular conversion in state-to-state transitions (e.g., glassy-to-rubbery, rubbery-to-melt, etc.) which were precisely interpreted.

Modeling background

The modeling stages depend on the number of polymer phases in the system. Accordingly, the temperature-dependent storage modulus of the neat polymer and nanocomposite samples can be predicted in one step while two different stages are required in the case of blend and BBN samples. For blend-based samples, the temperature-dependent storage modulus of the phases should be calculated separately, considering the impact of nanoparticles when present, and then combined. Besides, it is enough to define the molecular conversion degree in the case of neat and nanocomposite samples to predict the effect of temperature on the storage modulus of the system.

Defining the temperature dependency of the storage modulus

It is proved that the presence of nanoparticles in the polymer matrix substantially increases the impact of temperature on the storage modulus of the system [23, 34]. Accordingly, the temperature-dependent storage modulus of neat polymers and nanocomposites should be defined using different strategies based on the impact of nanoparticles on conversion degree of polymer molecules.

Neat polymer phase (without nanoparticles)

Bai et al. proposed the following equation to define the temperature-dependent storage modulus of the neat polymer matrix (E_p (T)) in the range of the glassy state to the melting point [35]:

$$E_p(T) = (1 - \alpha_g)E_g + \alpha_g(1 - \alpha_d)E_r \qquad (1)$$

where E_g and E_r are the storage moduli of the polymer matrix at glassy and rubbery states, respectively, and α_g and α_d denote the conversion degree of the glassy and decomposition transitions. The conversion rate in each state-to-state transition is definable as a function of activation energy, temperature and the content of un-converted polymer chains [35]:

$$\frac{d\alpha_g}{dt} = \psi_g(1 - \alpha_g)^n \qquad (2)$$

$$\frac{d\alpha_d}{dt} = \psi_d(1 - \alpha_d)^n \qquad (3)$$

where $\psi_g = A_g \exp(-E_{A,g}/RT)$ and $\psi_d = A_d \exp(-E_{A,d}/RT) = A_d\exp(E_{A,d}/RT)$ (A_g and A_d are Arrhenius's pre-exponential factors, $E_{A,g}$ and $E_{A,d}$ denote the activation energies related to each transition). Parameter n is representative of the reaction order and defines the impact of the content of un-converted polymer chains on the overall conversion rate. This parameter also adjusts the variation pattern of the model predictions with the actual DMTA results (Fig. 1). Integrating Eqs. (2 and 3) results in different temperature-dependent conversion degrees, with data regarding the pre-exponential factors and activation energies are available [35]. Indeed, Bai et al. use the Coats-Redfern method to solve Eqs. (2 and 3) to calculate the temperature-dependent pre-exponential factors and constant activation energies based on the experimentally obtained conversion degrees [36]. However, this method is considerably useful in explaining the transition kinetics of the polymer chains during heating a polymer material, it cannot provide direct results for α_g and α_d. To overcome this drawback, a specific strategy is proposed based on the developed form of the percolation theory which simply provides the required data regarding the temperature-dependent conversion degree of polymer molecules using only the values of storage modulus at different temperatures. Accordingly, the temperature-dependent storage modulus of a neat polymer phase in specific ranges can be defined by rearranging Eq. (1):

$$E_p(T) = (1 - \alpha_T)E_0 + \alpha_T E_f \qquad (4)$$

where α_T denotes the overall temperature-dependent conversion degree in the range of T_0 to T_f, E_0 and E_f represent the storage moduli at the beginning and end of the interval, respectively. Figure 1 represents the method to define different ranges from T_0 to the end of the following transition zone at T_f. As it is clear, the diagram is divided into different intervals, with concave or convex shapes, in which parameter n acquires different values (this is further discussed in "Results and discussion" section).
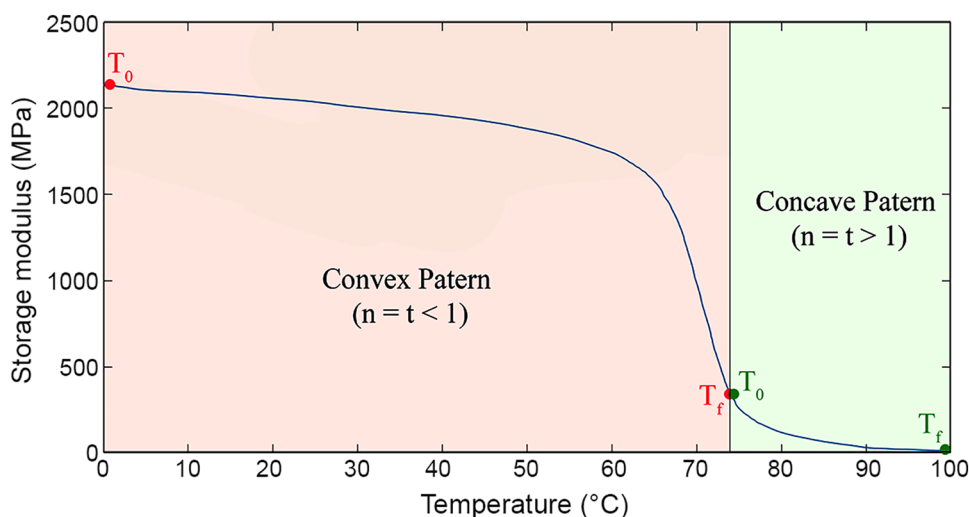
Polymer phase containing nanoparticles

As it is mentioned already, the formation of interphase around the nanoparticles can substantially affect the physical/mechanical characteristics of the system. Accordingly, Eq. (4) was developed considering the impact of nanoparticles on the polymer matrix. It is previously proposed that the conversion of polymer chains trapped in the polymer/particle interphase can be neglected during the transitions phenomenon (e.g., glassy-to-rubbery, rubbery-to-melt, etc.) and accordingly, the remained content of the polymer matrix that undergoes the state-to-state transition (φ_m) should be defined as follows [34]:

$$\varphi_m = 1 - (\varphi_n + \varphi_i) \qquad (5)$$

where φ_n and φ_i denote the volumetric content of the initially added nanoparticles and polymer/particle interphase region. Generally, the polymer/particle interphase is formed

Fig. 1 Method to define different intervals in a DMTA graph based on the concave and convex shapes of the related curve

due to the attraction of the adjoining polymer chains onto the surface of the nanoparticles. According to De Gennes's self-similar carpet theory, there is a distance-dependent concentration variation in the interphase region which suggests that the compactness of the attracted polymer chains is the highest on the surface and gradually decreases, based on a specific pattern, until it is equal to that of polymer matrix [37]. We have previously proved that those chains involved in the interphase region are affected by the superficial attraction energy of nanoparticles and can no longer act like other chains inside the polymer bulk [34]. This also includes their contribution to state-to-state transitions where the attraction energy of nanoparticles suppresses the induced thermal energy and does not let the conversion happen in the region.

It is reported that the gyration radius can be considered as the maximum thickness of the interphase region based on the molecular characteristics of the polymer chains [38, 39]:

$$\left\langle R_g^2 \right\rangle = \frac{\overline{M}_n C_\infty l^2}{M_{unit} 6}, \tag{6}$$

where $\overline{M}_n$ and M_{unit} denote the number average molecular weight and molecular weight of the repeating unit of the polymer chains. C_∞ is the Flory's characteristics ratio and l represents the C–C bond length. To estimate the content of the interphase region (φ_i), it is possible to use De Gennes's self-similar carpet theory which defines the concentration variation of the adsorbed polymer chains onto the surface of an adsorbent, as follows [37]:

$$C_i(z) \approx \left(\frac{z}{b}\right)^{\frac{1}{v}-3}, \tag{7}$$

where z is the distance from the surface, b denotes the Khun length of the polymer chains ($b = C_\infty l \sin((\pi - \alpha)/2)$ in which α is the angle between tetrahedral bonds) and v represents the scaling parameter. Using Eq. (7), it is possible to calculate the density variation per Khun length of the polymer chains in the interphase region, from the surface of the nanoparticles to the gyration radius of the chains:

$$\rho_i(z) = \frac{\rho_m}{b} \left(\frac{z}{b}\right)^{\frac{-(3v-1)}{v}}. \tag{8}$$

As it is clear, the density tends to infinity at $z = 0$ which is not a real case and accordingly, the lower bound of the integral (Eq. 9), used to calculate the average density of the interphase region ($\overline{\rho}_i$), should be set at a significantly small value such as βR_g ($\beta \to 0$):

$$\overline{\rho}_i = \int_{\beta R_g}^{R_g} \frac{\rho_m}{b} \left(\frac{z}{b}\right)^{\frac{-(3v-1)}{v}} dz = \frac{v}{1-2v}\rho_m\left(\left(\frac{R_g}{b}\right)^{\frac{1}{v}-2} - \left(\frac{\beta R_g}{b}\right)^{\frac{1}{v}-2}\right) \tag{9}$$

Accordingly, using the content and physical characteristics of the polymer phase, nanoparticles and polymer/particle interphase region, the volumetric content of the polymer phase which can undergo state-to-state transition (φ_m) can be calculated as follows:

$$\varphi_m = \frac{\rho_t\left(w_p \rho_n D_n^3 - w_n \overline{\rho}_i\left((2R_g + D_n)^3 - D_n^3\right)\right)}{\rho_p \rho_n W_t D_n^3} \tag{10}$$

where w_p and w_n are the weights of initially added polymer and nanoparticles, respectively. D_n denotes the diameter of the spherical nanoparticles, ρ_p represents the density of the polymer matrix in which the nanoparticles are dispersed, ρ_n is the density of nanoparticles, ρ_t and W_t represent the total density and weight of the polymer phase containing nanoparticles. It should be noted that Eq. (10) should be rearranged if the nanoparticles have any shapes other than spherical.

To calculate the temperature-dependent storage modulus of the polymer phase containing nanoparticles ($E_n(T)$), Eq. (4) can be developed based with φ_m as follows:

$$\varphi_m E_n(T) = \left(\varphi_m - \alpha_T'\right)E_0 + \alpha_T' E_f \tag{11}$$

where, α_T' denotes the overall conversion degree of polymer matrix containing nanoparticles.

Developing of percolation theory to calculate overall conversion degrees

Considering a polymer matrix as a blend of converted and un-converted molecules in the transition region, it is possible to use the percolation theory to define the storage modulus of the system as follows [34]:

$$E_b \approx E_{con.}\left(\alpha_i - \alpha_{cr}\right)^t \tag{12}$$

where E_b is the storage modulus of the blend, $E_{con.}$ denotes the storage modulus of the un-converted phase, α_i represents the temperature-dependent conversion degree and α_{cr} is the critical conversion degree which is significantly small. It is proved that the power, t, is equal to parameter $n (t = n)$, Eqs. 2 and 3, and therefore, the overall conversion degrees for the neat polymer phases with/without nanoparticles can be stated using Eqs. (13 and 14), respectively:

$$\alpha_T = \left(\frac{E_0 - E(T)}{E_0 - E_f}\right)^{\frac{1}{t}} \tag{13}$$

$$\alpha_T' = \varphi_m\left(\frac{E_0 - E(T)}{E_0 - E_f}\right)^{\frac{1}{t}} \tag{14}$$

where E(T) denotes the temperature-dependent storage modulus of the sample. As it is clear, the main parameters of Eqs. (13 and 14) should be defined using experimental results and accordingly, different characteristics of the system (e.g., dispersion quality of the nanoparticles, crystallinity, etc.) are simultaneously reflected in them.

Combining the temperature-dependent storage moduli of different phases in blend and BBN systems

The variation of the temperature-dependent storage modulus of the blend and BBN systems should be defined considering different parameters such as the content of constituents (e.g., major and minor polymer phases, nanoparticles), the localization of the nanoparticles and their probable impact on the interaction between the polymer phases. Accordingly, a developed form of the rule of mixtures was used to combine the obtained results of Eqs. (4 and 11) based on the volume fraction of the polymer phases:

$$E(T) = \left(1 - c_i \varphi_2\right) E_p(T) + c_i \varphi_2 E_n(T) \tag{15}$$

where E(T) is the temperature-dependent storage modulus of the blend or BBN system, φ_2 denotes the volumetric content of the minor polymer and c_i is a model parameter that represents the quality of the interaction between the polymer phases. It should be noted that $c_i = 1$, $c_i < 1$ and $c_i > 1$ represent normal, weakened and strengthened polymer/polymer interface, respectively. It was found that c_i can be assumed as 1 for polymer blends while for BBN samples it was in the range of 0.5–2.

It should be noted that, the combination of Eqs. (4, 11 and 15) results in defining the temperature-dependent storage modulus of the BBN systems (E(T)). However, for simple blends, without nanoparticles, Eq. (4) can be used to determine the temperature-dependent storage modulus of both phases and the results can be inserted in Eq. (15). Similarly, if the nanoparticles are dispersed in both major and minor phases the temperature-dependent storage modulus of both phases is definable using Eq. (11) and the obtained results can be combined using Eq. (15).

Defining the impact of nanoparticles on percolation threshold of the minor polymer phase in BBN systems

As mentioned earlier, the morphology of polymer blends is directly dependent on the compatibility and content of the phases. Also, the percolation threshold is reported as a quantitative parameter that defines a boundary between

droplet-matrix and combined droplet-matrix/co-continuous morphology [19]. The application of nanoparticles in BBN may affect the percolation threshold and accordingly, it is important to investigate the probable variation of the morphology in BBN after adding a specific amount of nanoparticles.

The percolation threshold for the dispersed nanoparticles in a polymer matrix (φ_{cr}) can be calculated as follows [40]:

$$\varphi_{cr} = \frac{V_{filler}}{V_{EV}} \tag{16}$$

where V_{filler} denotes the volume of an individual filler particle and V_{EV} denotes the volume of an excluded cubic volume containing the particle at its center. Similarly, it is possible to define the percolation threshold in binary polymer blends based on the concept of excluded volume (EV) in a binary polymer blend (Fig. 2).

It is assumed that the droplet of a dispersed polymer phase, with an average radius of r, is placed at the center of a cube, with a side length of $2(\xi + r)$, and the blend system consists of a specific number of these EVs (Fig. 2b). The percolation threshold of the polymer materials (φ_{crP}) is commonly considered in the range of 14–16% (by vol) which would be possible to theoretically calculate the value of parameters ξ at the percolation threshold (ξ_{cr})

($\xi_{cr} = r_{cr}\left(1.387\varphi_{crP}^{-1/3} - 1\right)$, r_{cr}, is the average radius of the droplets of the minor polymer phase at the percolation threshold) [10, 19]. Parameter r_{cr} can be defined using experimental approaches such as the FE-SEM test. It should be noted that parameter ξ_{cr} was not used in any represented model equation and its introduction is merely to address the physical meaning of the geometrical characteristics of the EVs.

The dispersion of nanoparticles in either of minor or major phase of a polymer blend is expected to have distinct impacts on the variation of the percolation threshold. The dispersion of the nanoparticles in the minor phase increases both parameters r_{cr} and ξ_{cr} in the excluded volume (Fig. 2b) based on which the new percolation threshold (φ_{crN}) can be defined as follows:

$$\varphi_{crN} = \frac{V_t \frac{4}{3}\pi\left(\varphi_n + \varphi_2\right)}{8V_2\left(1 + \left(1.387\varphi_{crP}^{-1/3} - 1\right)\right)^3 + V_t \frac{4}{3}\pi\varphi_n} \tag{17}$$

where V_t is the total volume of the system, V_2 and φ_2 denote the volume and volumetric content of the minor polymer phase and φ_{cr} is the percolation threshold of the neat blend, without nanoparticles. On the other hand, when the nanoparticles are dispersed in the major phase of the EV, parameter r remains constant while ξ_{cr} increases significantly. In this condition φ_{crN} can be stated as follows:

Fig. 2 a Hypothetical structure of a polymer blend containing a finite number of excluded volumes (EVs) and **b** the geometrical structure of an EV containing the sphere of dispersed polymer phase, with an average radius of *r*, at its center
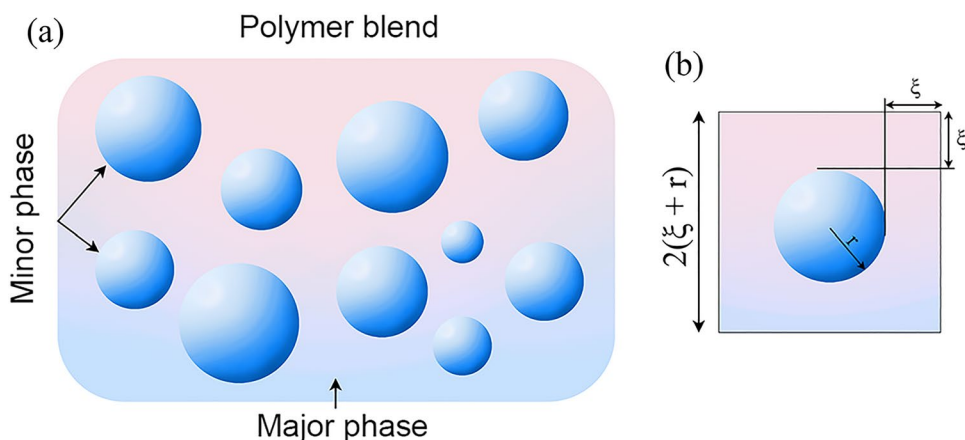
$$\varphi_{\text{crN}} = \frac{V_t \frac{4}{3}\pi\varphi_n}{8V_2\left(1 + \left(1.387\varphi_{\text{crP}}^{-1/3} - 1\right)\right)^3 + V_t \frac{4}{3}\pi\varphi_n} \qquad (18)$$

Based on Eqs. (17 and 18), it can be concluded that increasing the content of dispersed nanoparticles in the minor polymer phase increase the percolation threshold while increasing the content of dispersed nanoparticle in the major phase decreases φ_{crN}. It is proved that the presence of nanoparticles in either major or minor phases alters the polymer/polymer interfacial tension [41]. On the other hand, the dispersed nanoparticles can change the viscosity ratio of phases and accordingly, affect the coalescence phenomenon of the droplets at the percolation threshold [41]. Indeed, nanoparticles act as strong joints which decrease the mobility of the polymer chains, via forming polymer/particle interphase, and accordingly, the higher the content of compatible nanoparticles the less the mobility of polymer chains [42]. As a result, it can be concluded that the dispersion of a specific amount of nanoparticles (say Q grams) in the minor phase increases the percolation threshold since, besides affecting the interfacial tension, the dispersed droplets require more bulk to be able to move and coalesce, compared to pure droplets [41]. The same amount of nanoparticles (Q grams) may have less effect on the rheological behavior of the major phase, due to its higher volumetric content, while they can still significantly increase the polymer/polymer interfacial tension and facilitate the coalescence of the droplets of the minor polymer phase which lowers the percolation threshold [41].

Experimental

Materials

Sulfuric acid (H_2SO_4, 95–97%) and graphene oxide powder (density: 1.89 g cm^{-3}) were purchased from Merck Millipore and Sigma Aldrich corporations, respectively. Polyethylene terephthalate (PET, T_m 250 °C, 1.68 g cm^{-3}, Sigma Aldrich Co.) and high-density polyethylene (HDPE, 140 °C, 0.95 g cm^{-3}, KRP Co.) were used as received.

Synthesis of hollow graphene oxide (hGO) nanoparticles

Synthesis of hGO nanoparticles was performed based on a previously proposed strategy [25, 43]. Accordingly, 2 g of graphene oxide powder was added to 50 mL of DM water and the suspension was sonicated for 30 min. Further, H_2SO_4 was mixed with the obtained mixture until its concentration reached 1 M. After intensive agitation for 20 min, 35 mL of the final graphene oxide/water/H_2SO_4 suspension was poured into a Teflon-lined autoclave (50 mL). An oven was used to increase the temperature to 195 °C for 10 h which triggered the formation of hGO nanoparticles based on the aggregation of graphene powder around the formed CO_2, H_2, and CO bubbles [44]. The obtained products were collected using the centrifugation process and washed several times with DM water to remove all excessive materials.

Preparation of blend-based nanocomposite (BBN) samples

A Brabender internal mixer was used to prepare the required samples containing different amounts of constituent phases (process temperature: 250 °C, rotating speed: 60 rpm). Accordingly, in the case of BBN and blend samples, specific amounts of polymer phases were first mixed and then, the nanoparticles were added to the system. The characteristics of the prepared samples can be found in Table S1. The content of the polymer phases and nanoparticles were adjusted based on the presumed percolation threshold in the blend samples (15% by vol) so the impact of morphological

variation and amount of nanoparticles on the temperature-dependent storage modulus could be evaluated. The percolation threshold in most of the polymer blends is theoretically considered in the range of 14–16% (by vol) based on which different morphologies of immiscible binary polymer blends are discussed (e.g., droplet-matrix under the percolation threshold, co-continuous at phase inversion point, combination of droplet-matrix and co-continuous between percolation threshold and phase inversion point) [19, 20]. Also, based on the nature of the hGO nanoparticles, different PET/hGO nanocomposite samples were prepared, under the aforementioned melt mixing process conditions, to investigate the exclusive impact of different amounts of nanoparticles on the temperature-dependent tensile modulus of the minor polymer phase. These samples are referred to as PET-hGO (1%), PET-hGO (2%) and PET-hGO (3%) which denote the constituents of the samples as well as the volumetric content of hGO nanoparticles.

Characterization

Field emission scanning electron microscopy (FE-SEM, MIRA3 Tescan) was used to evaluate the morphology of the prepared blend samples. The samples were first frozen using liquid nitrogen and were broken into small pieces, ready for coating with gold, before subjecting to the FE-SEM test. Fourier-transform infrared spectroscopy test (FTIR, Tensor 27, Bruker, 400–4000 cm^{-1}) was used to study the surface chemistry of the synthesized hGO nanoparticles and define their tendency to either minor or major phase (e.g., HDPE or PET phase). Also, to further evaluate the behavior of nanoparticles in the blend samples, a suspension of hGO nanoparticles in an oil–water dual-phase system was prepared and their dispersion in the polar or apolar phase was studied after stirring. Dynamic mechanical thermal analyses (DMTA)

were conducted using a Pyris Diamond testing device (Perkin Elmer, USA) in a temperature range of 0 °C to 100 °C and the results were used to validate the model predictions.

Results and discussion

According to Eq. (15), the temperature-dependent storage modulus of the BBN and blend samples can be assumed independent of the morphological variation and therefore, to validate this assumption it was crucial to investigate the impact of all blend morphologies on E(T). To this end, BN91, BN72, and BN55 blend samples, without nanoparticles, were subjected to FE-SEM test to ensure their different morphologies. Figure 3 represents the morphology variation in samples with increasing content of the minor polymer phase. BN91 sample including 10% (by vol) of PET was found to have droplet-matrix morphology (Fig. 3a) while the morphology of BN72, with 25% (by vol) of the minor polymer phase, was a combination of co-continuous and droplet-matrix (Fig. 3b). On the other hand, BN55 sample demonstrated co-continuous morphology at the so-called phase inversion point ($\varphi_2 = 0.5$) (Fig. 3c).

As it is mentioned before, the percolation threshold of the blend system can be differently affected by dispersion of the nanoparticles in either major or minor phases and consequently alter the morphology of the samples. Accordingly, it was necessary to define the polymer phase in which hGO nanoparticles could simultaneously disperse before evaluating their impact on the percolation threshold. Figure 4a represents the FTIR results of the synthesized hGO nanoparticles. The characteristics peaks at 877, 1471 and 2926 cm^{-1} denote the presence of C–H bond (bending vibration) [45, 46]. The peaks at 524 cm^{-1} (C–O–C), 1166 cm^{-1} (C–O), 1631 cm^{-1} (C=C) and 2854 cm^{-1} (C–H, stretching)
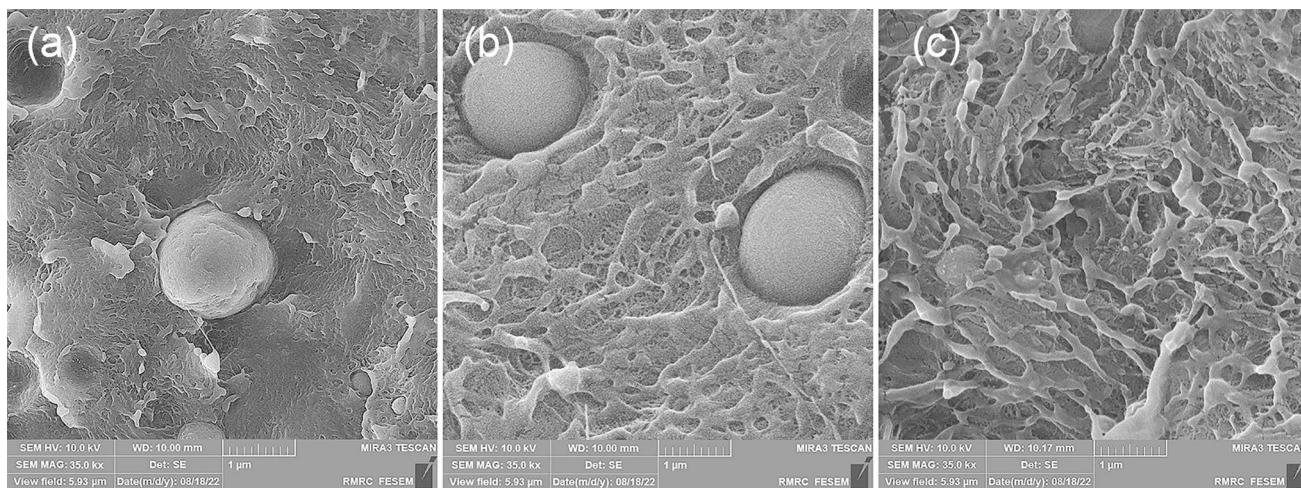

Fig. 3 FE-SEM results demonstrating the morphology of: **a** BN91, **b** BN72 and **c** BN55 blend samples

represent the common characteristic peaks of graphene oxide particles [46]. On the other hand, the appearance of strong peaks at 1089, 1732 and 3435 cm^{-1} denote the presence of C–OH, C=O and – OH functional groups, respectively, on the surface of nanoparticles which verify their higher compatibility with PET compared to HDPE [43]. To further ensure the polar nature of the nanoparticles, they were dispersed in an oil–water dual-phase system and stirred before setting to rest. As demonstrated in Fig. 4b almost all nanoparticles were localized in the polar phase. This confirmed the tendency of the synthesized hGO toward the PET phase, with higher polarity compared to HDPE. The instantaneous migration of hGO nanoparticles into the water phase, after stopping the agitation, is also represented in the Supplementary Video. Similar results are reported in the case of PS/PMMA blend-based nanocomposites according to which hGO nanoparticles, synthesized using the same previsously discussed method, disperse in PMMA phase, with higher polarity [25].

Therefore, considering the dispersion of hGO nanoparticles in the minor polymer phase, Eq. (17) was used to calculate the new percolation threshold based on the variations in nanoparticles content. The obtained results are represented in Table 1 according to which it was ensured that the presence of nanoparticles did not affect the morphology of BN91, BN72, and BN55 samples since the highest percolation threshold was below the volume fraction of the minor polymer phase in BN72 sample (25% by vol) (Fig. 3).

The DMTA test results of PET samples containing 0–3% (by vol) of hGO nanoparticles are represented in Fig. S2. As it is clear, hGO nanoparticles have significantly affected the temperature-dependent storage modulus of the polymer matrix at the glassy state as well as the glass transition region, ascribed to the formation of an interphase region and strong polymer/particle bounding [47]. It should be noted

that hGO nanoparticles are proved to be unique heat conductors and can facilitate heat transfer in the nanocomposite systems which negatively affects E(T) [48].

Figure 5 demonstrates the DMTA results and model predictions for BN91, BN72, BN55, HDPE, and PET samples. It is clear that the predictions of Eq. (4), regarding the temperature-dependent storage modulus of the neat HDPE and PET phases ($E_p(T)$), are acceptably accurate with a maximum error of 7%. Also, the predicted data for the blend samples (Eq. (15), $c_i = 1$) are close to the related experimental results, with a maximum error of 6%. According to the represented results in Fig. 5 and the morphological difference between the tested samples, it can be concluded that the model is not dependent on the morphological variation of the blend samples.

Based on Eqs. (13 and 14), the conversion degree in neat and nanocomposite polymer phases is a function of parameter t. As mentioned before, it is proved that $t = n$ which denotes the dependency of α_T and α'_T to the un-converted portion of the polymer molecules during different state-to-state transitions (Eqs. 2 and 3) [34]. Also, $t > 1$ and $t \leq 1$ cause the model predictions curve to make concave and convex shapes, respectively. This suggests that the conversion rate before and during state-to-state transition is mostly dependent on values of the activation energy and Arrhenius's pre-exponential factor. However, at the end of the transition

Table 1 Variation of percolation threshold with increasing the content of hGO in PET minor phase

	Nanoparticles content (% by vol)			
	0	1	2	3
Percolation threshold (% by vol)	0.15	0.21	0.22	0.23

Fig. 4 **a** FTIR results of the synthesized hGO nanoparticles and **b** the localization of hGO polar nanoparticles in the water phase
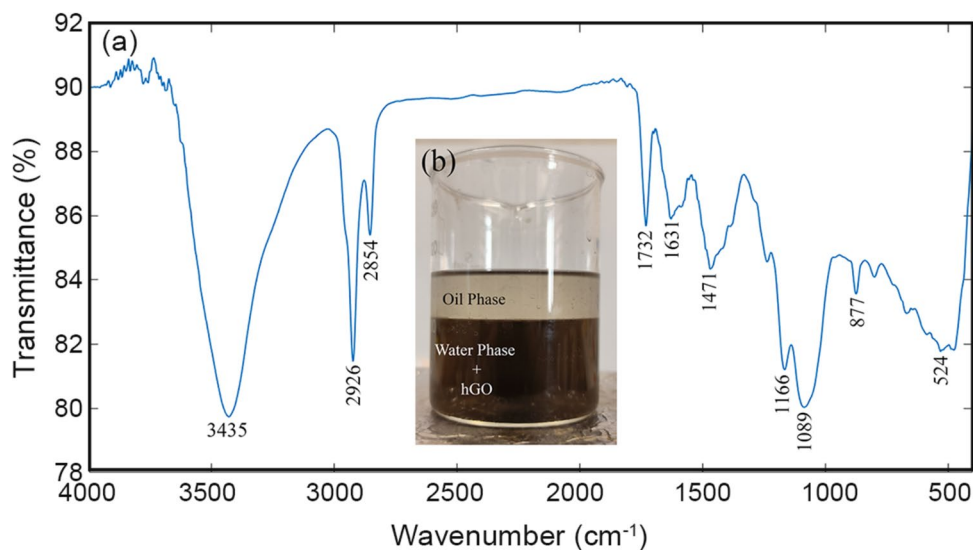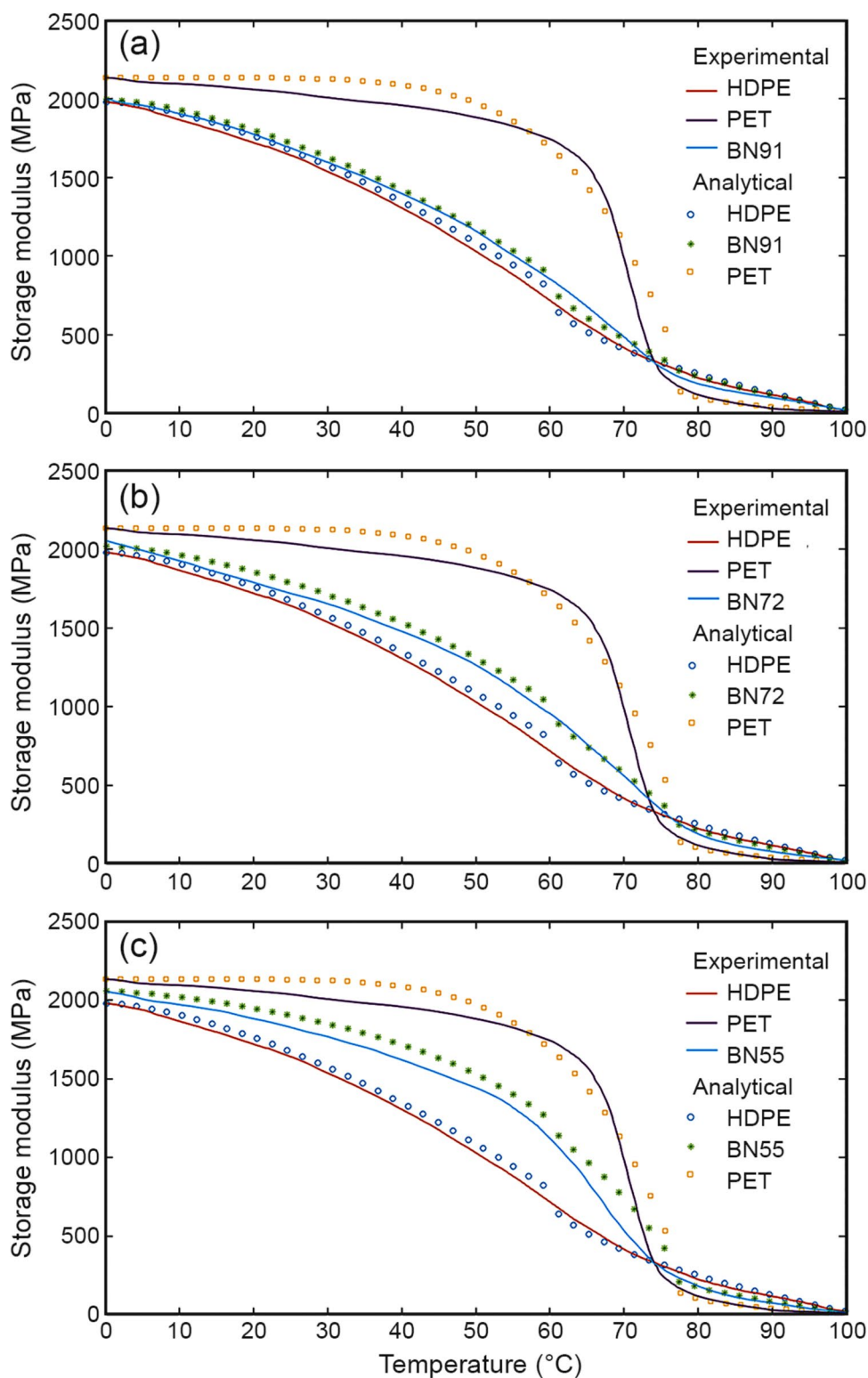
Fig. 5 DMTA experimental results and model predictions on pure PET, HDPE and **a** BN91, **b** BN72 and **c** BN55 blend samples

region, it is the amount of the un-converted polymer molecules which control the conversion rate. Table 2 represents the maximum and minimum adopted values of parameter, t, to obtain the best predictions considering the value of different conversion degrees. It can be seen that the value of t_{min}

at the beginning of the transition region is less than 1 for all samples which, as mentioned, denotes the substantial impact of activation energy of transition and Arrhenius's pre-exponential factor on the conversion rate. However, the values of t_{max}, at the end of transition zone, suggest the dependency

of the conversion rate of polymer molecules on the content of un-converted polymer molecules. Also, t_{min} of the minor polymer phase (PET) decreases with the content of nanoparticles which may be attributed to the formation of polymer/particle interphase and decrement of φ_m (Eq. 10). On the other hand, t_{max} of the PET-hGO samples increases with φ_n, until it is equal to t_{max} of pure PET, denoting the decrement of the impact of polymer/particle interphase region on the temperature-dependent storage modulus of the nanocomposites with increasing the nanoparticles content [28].

The DMTA test results and corresponding model predictions for BN721, BN722 and BN723 are represented in Fig. S3. The analytical results for all samples are acceptably close to the experimental data, with the highest point-by-point prediction error of $\cong 17\%$ for BN552 sample. It should be noted that the reported error value does not reflect the overall prediction error, but the maximum deviation of a theoretical result from only one particular actual data, at high temperatures (> 75 °C) due to the variation of interactions at the polymer/polymer interface [49]. The comparison of analytical and experimental data for BN91 and BN55 samples containing 1–3% (by vol) of nanoparticles are represented in Figs. S4 and S5, respectively.

As mentioned, parameter c_i represents the impact of the polymer/polymer interface on the mechanical characteristics of the system which may be affected by the temperature, content of minor polymer phase and nanoparticles. According to the concept of Pickering emulsions, a portion of the dispersed nanoparticles in a mixture of immiscible phases tend to migrate toward the interphase to decrease the internal energy of the system [50]. As it is illustrated in Fig. 6, there are some nanoparticles left at the HDPE/PET interface, after pulling out the PET sphere, which proves the occurrence of a similar phenomenon in the prepared BBN samples. Based on the summarized results in Table 3 and the value of c_i for pure blend samples ($c_i = 1$), it is clear that the presence of the hGO nanoparticles in the polymer minor phase substantially affects the mechanical interactions at the polymer/polymer interface. The obtained values for c_i in the case of all BBN samples based on BN72 blend are the highest and almost independent of the nanoparticles content. This reveals that the synthesized hGO nanoparticles had the best performance in the HDPE/PET blend around the percolation threshold. Also, the low c_i values of the BBN samples based on BN55

blend suggest that increasing the nanoparticles content in the system may result in their aggregation/agglomeration which negatively affects the mechanical characteristics of the polymer/polymer interface [10]. The same phenomenon can be seen in the case of BN91 sample containing 1% (by vol) of hGO nanoparticles which can be ascribed to the low content of nanoparticles and their weak dispersion in the PET phase (10% by vol) which causes the formation of aggregates/agglomerates. However, increasing the nanoparticles content, in BN912 and BN913 samples, could increase the mechanical characteristics of the polymer/polymer interface.

Figure 7 represents the impact of polymer/polymer interface on the accuracy of model predictions, based on the values of c_i (Table 3). As it is clear, the polymer/polymer interface has a slight impact on the obtained analytical results regarding the temperature-dependent storage modulus of the BBN samples based on BN91 blend (Fig. 7a). This can be attributed to the relatively low content of PET in the system,
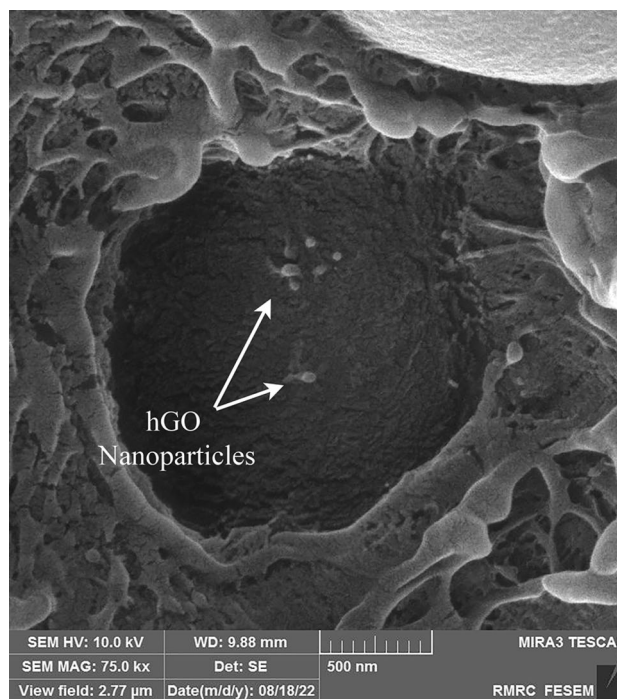

**Fig. 6** Residual hGO nanoparticles at the PET/HDPE interface after pulling out a PET sphere

Table 2 Maximum and minimum applied values for parameter t

Sample	t_{min}	t_{max}
PET	0.18	9
HDPE	0.65	2
PET-hGO(1%)	0.16	6
PET-hGO(2%)	0.14	7.5
PET-hGO(3%)	0.13	9

Table 3 Value of parameter c_i for different prepared samples (Eq. 15)

Blend samples	Nanoparticles content (% by vol)			
	0	1	2	3
BN91	1	0.8	1.3	1.35
BN72	1	2	1.8	2
BN55	1	0.71	0.8	0.85

Fig. 7 Impact of the polymer/polymer interface on the model predictions regarding the temperature-dependent storage modulus for **a** BN91, **b** BN72 and **c** BN55 samples containing 1–3% (by vol) of nanoparticles (temperature range of 0 to 100 °C)
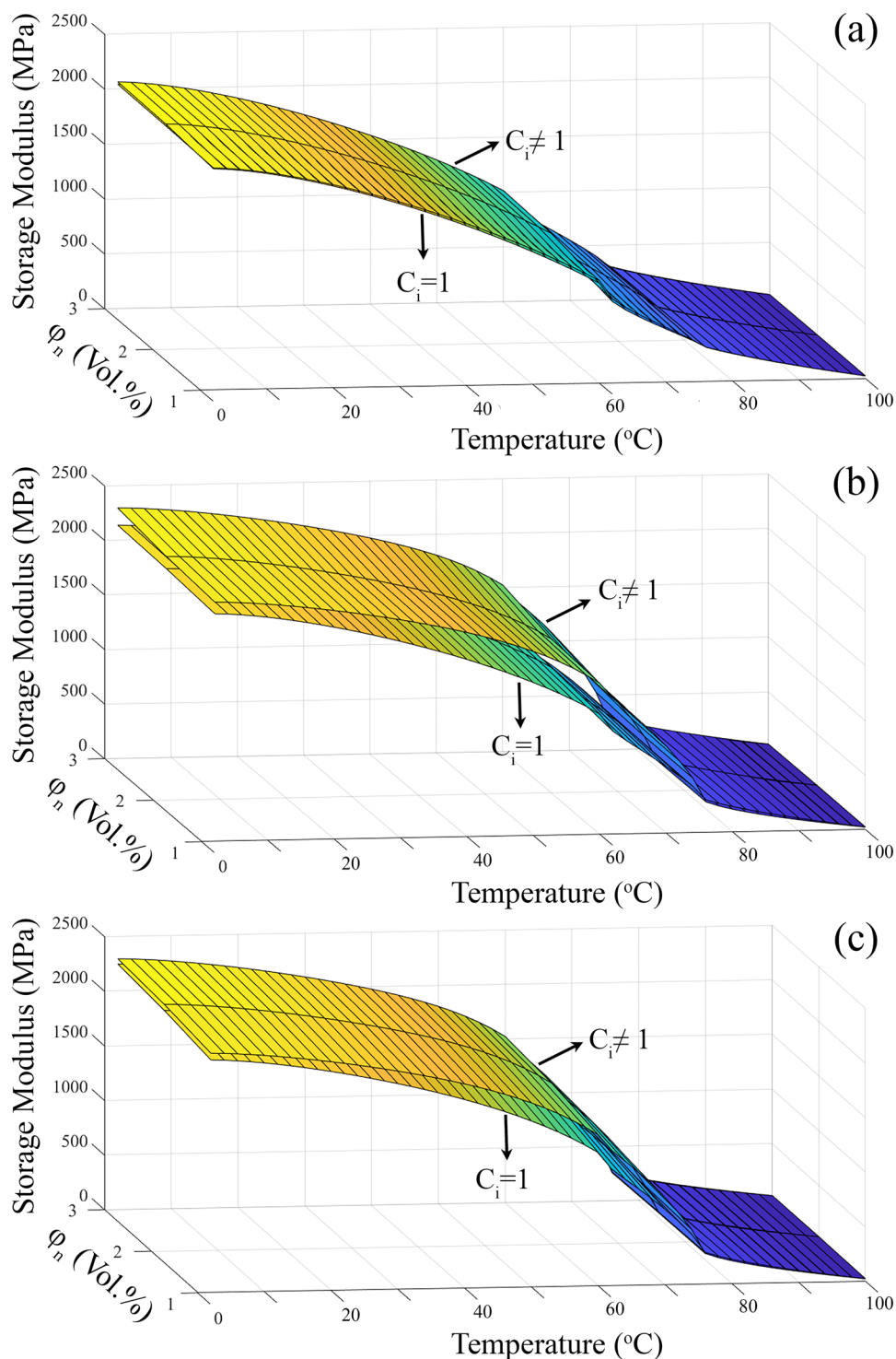
containing almost all the added nanoparticles, whose impact on the system is independent of the mechanical characteristics of the interface. On the other hand, comparing the results for the BBN samples based on BN72 and BN55 blends (Fig. 7b and c) shows that the effect of nanoparticles on the polymer/polymer interface is more significant around the percolation threshold of the minor polymer phase, which increased from 15% (by vol) to a maximum value of 23% (by vol) (Table 1). Moreover, according to the demonstrated Fig. 7b and c, the highest impact of the polymer/polymer interface in BBN samples should be expected in the state-to-state transition region where the conversion rate is proved to be dependent on the activation energy and Arrhenius's pre-exponential factor [34].

Conclusion

The analytical results showed that the developed percolation theory provided accurate results regarding the impact of temperature on the order of conversion rate as well as the conversion degree. The content of un-convertible polymer chains, forming the polymer/particle interphase region, in nanocomposite and blend-based nanocomposite samples was estimated using a developed form of De Gennes's theory considering the molecular and physical characteristics of the adsorbed polymer chains. This approach helped to highlight the difference between the variation of temperature-dependent storage modulus of neat polymers and polymer nanocomposites. Modeling the BBN system using the concept of excluded volumes was shown to be a useful method for defining the variation of the percolation threshold of the minor polymer phase due to the presence of nanoparticles. Coupling the related information of the results of morphology evaluations, using FE-SEM images, may confirm the independency of the proposed model from the morphological variations in BBN samples. The order of the conversion rate was denoted to have a significant effect on the model prediction accuracy based on which the dependency of the conversion rate to the related parameters was precisely interpreted. Involving the impact of the polymer/polymer interface in the analytical predictions was found to be a practical method to enhance the model accuracy in the case of blend and blend-based polymer nanocomposite samples. Optimizing the content of nanoparticles and minor polymer phase had also a significant impact on the characteristics of the interface and the accuracy of model predictions. As it is mentioned before, the volumetric content of the polymer chains which can undergo state-to-state conversion is directly dependent on the size and shape of nanoparticles which can be rearranged in the case of applying nanoparticles with any shapes other than spherical. Also, investigating the impact of specific nanoparticles, localized at the polymer/polymer interface, on the temperature-dependent characteristics of the BBN systems can be an interesting subject for further studies.

Supplementary Information The online version contains supplementary material available at https://doi.org/10.1007/s13726-024-01300-1.

Data availability The data that support the findings of this study are available from the corresponding author, upon reasonable request.

References

1. Misra A (2014) Applications of polymers in drug delivery. Smithers Information Limited, Shrewsbury
2. Chanda M, Roy SK (2008) Industrial polymers, specialty polymers, and their applications. New york, CRC
3. Mandelkern L (1985) The relation between structure and properties of crystalline polymers. Polym J 17:337–350
4. Dusunceli N, Colak OU (2008) Modelling effects of degree of crystallinity on mechanical behavior of semicrystalline polymers. Int J Plast 24:1224–1242
5. Hojatzadeh S, Sharifzadeh E, Rahimpour F (2023) An EBM based multi-stage mechanical model to predict the time-dependent creep behavior of semi-crystalline polymer nanocomposites. Mech Mater 184:104737
6. Hojatzadeh S, Rahimpour F, Sharifzadeh E (2023) A study on the synergetic effects of self/induced crystallization and nanoparticles on the mechanical properties of semi-crystalline polymer nanocomposites: experimental and analytical approaches. Iran Polym J 32:543–555
7. Paul DR, Barlow JW (1979) A brief review of polymer blend technology. In: Cooper SL, Estes GM (eds) Multiphase polymers. American Chemical Society, Washington
8. Thomas S, Ajitha AR, Jaroszewski M (2023) Polymer blend nanocomposites for energy storage applications. Elsevier Science, Amsterdam
9. Muhammed Shameem M, Sasikanth SM, Annamalai R, Ganapathi Raman R (2021) A brief review on polymer nanocomposites and its applications. Mater Today Proc 45:2536–2539
10. Sharifzadeh E, Maleki M (2022) An energy-based approach to study the aggregation/agglomeration phenomenon in polymer nanocomposites: dispersion force against inter-particle cohesion. Polym Compos 43:5145–5158
11. Macosko CW, Jeon HK, Hoye TR (2005) Reactions at polymer–polymer interfaces for blend compatibilization. Prog Polym Sci 30:939–947
12. Alkhodairi H, Russell ST, Pribyl J, Benicewicz BC, Kumar SK (2020) Compatibilizing immiscible polymer blends with sparsely grafted nanoparticles. Macromolecules 53:10330–10338
13. Sharifzadeh E (2019) Modeling of the mechanical properties of blend based polymer nanocomposites considering the effects of Janus nanoparticles on polymer/polymer interface. Chin J Polym Sci 37:164–177
14. Sharifzadeh E, Azimi N, Mohammadi R (2023) Improved thermostimulative shape memory behavior of HDPE/PET immiscible blend-based polymer nanocomposite using amphiphilic Janus nanoparticles. Polym Compos 44:1161–1174
15. Nofar M, Salehiyan R, Ray SS (2021) Influence of nanoparticles and their selective localization on the structure and properties of polylactide-based blend nanocomposites. Compos B Eng 215:108845
16. Su H, Hurd Price CA, Jing L, Tian Q, Liu J, Qian K (2019) Janus particles: design, preparation, and biomedical applications. Mater Today Bio 4:100033
17. Sharifzadeh E, Ghasemi I, Qarebagh AN (2015) Modeling of blend-based polymer nanocomposites using a knotted approximation of Young's modulus. Iran Polym J 24:1039–1047
18. Naffakh M, Díez-Pascual AM, Marco C (2016) Polymer blend nanocomposites based on poly(l-lactic acid), polypropylene and WS2 inorganic nanotubes. RSC Adv 6:40033–40044
19. Wang JF, Carson JK, North MF, Cleland DJ (2010) A knotted and interconnected skeleton structural model for predicting Young's modulus of binary phase polymer blends. Polym Eng Sci 50:643–651
20. Sharifzadeh E, Ghasemi I, Karrabi M, Azizi H (2014) A new approach in modeling of mechanical properties of binary phase polymeric blends. Iran Polym J 23:525–530
21. Seymour R (2012) Applications of polymers. Springer, Denver
22. Ahmad N, Zhang X, Yang S, Zhang D, Wang J, Zafar SU, Li Y, Zhang Y, Hussain S, Cheng Z, Kumaresan A, Zhou H (2019) Polydopamine/ZnO electron transport layers enhance

charge extraction in inverted non-fullerene organic solar cells. J MaterChem C. 7:10795–10801

23. Sharifzadeh E, Cheraghi K (2021) Temperature-affected mechanical properties of polymer nanocomposites from glassy-state to glass transition temperature. Mech Mater 160:103990

24. Godovsky YK (2012) Thermophysical properties of polymers. Springer, Berlin

25. Pourakbar E, Sharifzadeh E (2021) Synthesis of Janus/non-Janus hollow graphene oxide micro- and nanoparticles and the effects of their localization on the thermal conductivity of blend-based polymer composites. J Mater Sci 56:18078–18092

26. Huang C, Qian X, Yang R (2018) Thermal conductivity of polymers and polymer nanocomposites. Mater Sci Eng R Rep 132:1–22

27. Ahmad N, Liang G, Fan P, Zhou H (2022) Anode interfacial modification for non-fullerene polymer solar cells: recent advances and prospects. InfoMat 4:e12370

28. Sharifzadeh E (2021) Evaluating the dependency of polymer/particle interphase thickness to the nanoparticles content, aggregation/agglomeration factor and type of the exerted driving force. Iran Polym J 30:1063–1072

29. Huang J, Zhou J, Liu M (2022) Interphase in polymer nanocomposites. JACS Au 2:280–291

30. Ghadami H, Sharifzadeh E, Azimi N (2023) A scaling theory to approximate the thermal conductivity of the interphase region in polymer nanocomposites. J Reinf Plast Compos 1:07316844231197266

31. Singh M, Chandra Pandey J (2022) Probing thermal conductivity of interphase in epoxy alumina nanocomposites. Polym Polym Comps 30:09673911221077489

32. Bansal A, Yang H, Li C, Benicewicz BC, Kumar SK, Schadler LS (2006) Controlling the thermomechanical properties of polymer nanocomposites by tailoring the polymer–particle interface. J Polym Sci B Polym Phys 44:2944–2950

33. Ahmad N, Zhao Y, Ye F, Zhao J, Chen S, Zheng Z, Fan P, Yan C, Li Y, Su Z, Zhang X, Liang G (2023) Cadmium-free Kesterite thin-film solar cells with high efficiency approaching 12%. Adv Sci 10:2302869

34. Sharifzadeh E, Mohammadi R (2021) Temperature-/frequency-dependent complex viscosity and tensile modulus of polymer nanocomposites from the glassy state to the melting point. Polym Eng Sci 61:2600–2615

35. Bai Y, Keller T, Vallée T (2008) Modeling of stiffness of FRP composites under elevated and high temperatures. Compos Sci Techol 68:3099–3106

36. Coats AW, Redfern JP (1964) Kinetic parameters from thermogravimetric data. Nature 201:68–69

37. De Gennes PG (1976) Scaling theory of polymer adsorption. J Phys 37:1445–1452

38. Zare Y, Rhee KY (2017) Development of a conventional model to predict the electrical conductivity of polymer/carbon nanotubes nanocomposites by interphase, waviness and contact effects. Compos Part A Appl Sci 100:305–312

39. Ader F, Sharifzadeh E, Azimi N (2023) A novel strategy to predict the tensile strength of polymer/particle interphase based on De Gennes's self-similar carpet theory. Polym Eng Sci 1:1–9

40. Tang Z-H, Li Y-Q, Huang P, Fu Y-Q, Hu N, Fu S-Y (2021) A new analytical model for predicting the electrical conductivity of carbon nanotube nanocomposites. Compos Commun 23:100577

41. Salzano de Luna M, Filippone G (2016) Effects of nanoparticles on the morphology of immiscible polymer blends: challenges and opportunities. Eur Polym J 79:198–218

42. Ader F, Sharifzadeh E (2021) Rheological and mechanical behavior of blend-based polymer nanocomposites containing Janus and non-Janus silica nanoparticles. Colloid Polym Sci 299:1843–1852

43. Sharifzadeh E, Parsnasab M (2021) Direct and reverse desymmetrization process in O/W pickering emulsions to produce hollow graphene oxide Janus micro/nano-particles. Colloid Surf A Physicochem Eng Asp 619:126522

44. Cao J, Wang Y, Xiao P, Chen Y, Zhou Y, Ouyang J-H, Jia D (2013) Hollow graphene spheres self-assembled from graphene oxide sheets by a one-step hydrothermal process. Carbon 56:389–391

45. Valencia C, Valencia CH, Zuluaga F, Valencia ME, Mina JH, Grande-Tovar CD (2018) Synthesis and application of scaffolds of chitosan-graphene oxide by the freeze-drying method for tissue regeneration. Molecules 23:2651

46. Sharma N, Sharma V, Jain Y, Kumari M, Gupta R, Sharma SK, Sachdev K (2017) Synthesis and characterization of graphene oxide (GO) and reduced graphene oxide (rGO) for gas sensing application. Macromol Symp 376:1700006

47. Bitenieks J, Merijs Meri R, Zicans J, Buks K (2020) Dynamic mechanical, dielectrical, and rheological analysis of polyethylene terephthalate/carbon nanotube nanocomposites prepared by melt processing. Int J Polym Sci 2020:5715463

48. Ader F, Sharifzadeh E (2022) Investigating the effects of hollow graphene oxide nanoparticles on the thermal/mechanical properties of polymer nanocomposites: experimental, analytical and simulation approaches. IJChE 18:71–83

49. Xavier P, Rao P, Bose S (2016) Nanoparticle induced miscibility in LCST polymer blends: critically assessing the enthalpic and entropic effects. Phys Chem Chem Phys 18:47–64

50. Gonzalez Ortiz D, Pochat-Bohatier C, Cambedouzou J, Bechelany M, Miele P (2020) Current trends in pickering emulsions: particle morphology and applications. Engineering 6:468–482